JBC Papers in Press. Published on July 27, 2014 as Manuscript M114.558817
The latest version is at http://www.jbc.org/cgi/doi/10.1074/jbc.M114.558817

Phospholipase D Facilitates Efficient Entry of Influenza Virus Allowing Escape from Innate Immune Inhibition

Thomas H. Oguin III[1,2], Shalini Sharma[3], Amanda D. Stuart[4], Susu Duan[1], Sarah A. Scott[5], Carrie K. Jones[5,8], J. Scott Daniels[5,8], Craig W. Lindsley[5,6,8], Paul G. Thomas[1], and H. Alex Brown[5,6,7*]**

[1]Department of Immunology, St. Jude Children's Research Hospital, Memphis, TN 38105-3678, USA, [2]Department of Biological Sciences, University of Memphis, Memphis, TN 38152, USA, [3]Department of Veterinary Physiology and Biochemistry, Lala Lajpat Rai University of Veterinary and Animal Sciences, Hisar- 125004 , Haryana, India [4]Department of Pathology, University of Cambridge, Cambridge, UK CB2 1QP,[5]Department of Pharmacology, Vanderbilt University Medical Center, Nashville, TN 37232-6600, USA,[6]Department of Chemistry and The Vanderbilt Institute of Chemical Biology, Vanderbilt University, Nashville, TN 37232, USA, [7]Department of Biochemistry, Vanderbilt University Medical Center, Nashville, TN 37232-6600, USA, [8]Vanderbilt Center for Neuroscience Drug Discovery, Vanderbilt University Medical Center, Nashville, TN 37232-0697, USA. [8]

*Running title: *PLD in influenza replication and defense evasion*

To whom correspondence should be addressed: H. Alex Brown*, Department of Pharmacology, Vanderbilt University Medical Center, Vanderbilt University, Nashville TN 37232, USA, Tel.: (615)936-3888, E-mail: alex.brown@vanderbilt.edu; Paul G. Thomas**, Department of Immunology, St. Jude Children's Research Hospital, Memphis, TN 38105, USA, Tel.: (901)595-6507, E-mail: Paul.Thomas@stjude.org

Keywords: Phospholipase D, influenza, small molecule inhibitors, antiviral, innate immunity, lipid signaling.

Background: Identifying host factors used by influenza can aid in the defense against pandemics that threaten public health.
Results: Phospholipase D (PLD) contributes to viral infection and innate immune evasion strategies.
Conclusion: Inhibition of PLD activity reduces influenza reproduction.
Significance: PLD inhibition presents a novel approach to restrict influenza infection and viral escape.

ABSTRACT

Lipid metabolism plays a fundamental role during influenza virus replication, although key regulators of lipid-dependent trafficking and virus production remain inadequately defined. This report demonstrates that infection by influenza virus stimulates phospholipase D (PLD) activity and PLD co-localizes with influenza during infection. Both chemical inhibition and RNA interference of PLD delayed viral entry and reduced viral titers *in vitro*. Although there may be contributions by both major isoenzymes, the effects on viral infectivity appear to be more dependent on the PLD2 isoenzyme. *In vivo*, PLD2 inhibition reduced virus titer and correlated with significant increases in transcription of innate antiviral effectors. The reduction in viral titer

downstream of PLD2 inhibition was dependent on RIG-I, IRF3, and MxA, but not IRF7. Inhibition of PLD2 accelerated the accumulation of MxA in foci as early as 30 minutes post-infection. Together these data suggest that PLD facilitates the rapid endocytosis of influenza virus, permitting viral escape from innate immune detection and effectors that are capable of limiting lethal infection.

Lipid species play integral roles in cellular signaling and intracellular trafficking. Influenza viruses exploit these fundamental processes within the host cell to facilitate entry and subsequently drive virus replication. The cycle begins with the viral surface protein hemagglutinin (HA)[9] binding to an epithelial cell surface sialic acid moiety. Typically, this triggers endocytosis, allowing the virus entry inside the host cell, incorporating itself within the host membrane. As the endosome matures, acidification initiates a conformational change in the HA allowing it to fuse with the host endosomal membrane and release the ribonucleoprotein complexes, which are trafficked to the nucleus where RNA-dependent polymerases replicate the viral genome and make the mRNA for viral proteins. After proteins are synthesized, they accumulate at the cell membrane, complex with viral genomes, and bud off the cell surface, forming the viral envelope from the host cell membrane. Lipids are fundamentally involved both in the entry and egress of the virus (1).

In addition to playing structural roles in viral entry and budding, lipid species also serve as intra- and extra-cellular signals as part of the innate immune response. 25-hydroxycholesterol is secreted by macrophages in response to the Stat1/IFN pathway and can promote resistance to multiple viruses (2). Protectin D1 was identified as promoting an anti-inflammatory state that alleviated severe disease in an H5N1 infection (3). The 12/15 lipoxygenase pathway that generates protectin D1 was identified in another screen as being associated with mild infection in both mice and humans (4). PI3K has been demonstrated to have a role in influenza infection and host defense (5). The lipid binding protein Epsin-1 is a regulator of clathrin-mediated endocytosis of influenza virus (6). Lipid rafts also are involved in influenza virus (7) and HIV replication (8). Clearly, lipid species are influencial during viral pathogenesis and present a ripe opportunity for further research.

Despite recent findings on the participation of sterols, arachidonic acid derived species and lipid structures (such as rafts) in the regulation of influenza infection, the roles of glycerophospholipids have been ill defined. PLD enzymes play critical roles in generating lipid signaling molecules and contributing to membrane structure. The primary lipid product of PLD, phosphatidic acid (PA), is an important bioactive lipid that is involved in membrane biogenesis and curvature, in addition to being a second messenger in signaling pathways (9,10). Specifically, PA can be converted into diacylglycerol by phosphatidic acid phosphohydrolase, which subsequently activates protein kinase C (PKC) and other signaling proteins. Prior studies demonstrated that inhibiting PKC activity during influenza infection interferes with intracellular trafficking of the virus and protects cells from infection (11). Thus, PLD appears to be a potential targetable candidate as a host restriction factor of influenza virus replication.

In mammals, two predominant isoenzymes, PLD1 and PLD2, are well characterized. Recently, PLD isoform-preferring inhibitors have been designed, synthesized, and characterized (12,13). The development of these PLD inhibitors has facilitated the interrogation of the specific role of isoenzymes in various cellular processes (14). Utilizing these novel synthetic compounds and other biochemical approaches, the upregulation of PLD activity during influenza infection is demonstrated, in addition to evidence that PLD inhibition delays virus entry, allowing for a more robust innate antiviral response to be mounted in the infected host cell, leading to a significant reduction in viral titer. Consequently, PLD is a targetable host restriction factor for influenza viruses that facilitates rapid endosomal trafficking and innate immune escape in the host cell.

EXPERIMENTAL PROCEDURES

Chemical synthesis and purification - PLD isoenzyme-preferring inhibitors were synthesized

and characterized as described in detail previously (12,13).

Mass spectrometry-based lipid analysis - For analysis of cellular lipids, A549 cells were serum starved for 1 hour, infected at 1 MOI with influenza A/California/04/2009 or other indicated strains, and then maintained in 6-well plates for the indicated treatment times. Mock infected and influenza A infected cells were harvested at indicated times after infection and administration of PLD inhibitors. To extract phospholipids, ~1x10^6 cells were washed with ice-cold PBS, scraped into 1 ml of ice-cold PBS, and aliquots were taken for protein analysis. After centrifugation and PBS aspiration, the pellet was extracted by a modified Bligh and Dyer method using 800 µl ice-cold 0.1 N HCl: CH_3OH (1:1) and 400 µl of ice-cold $CHCl_3$ (15). Following vortexing for 1 min at 4 °C phases were separated by centrifugation (18,000 × g for 5 min, 4 °C). The lower organic layer was isolated, synthetic odd-carbon phospholipids (four per phospholipid class) were added as standards, and the solvent was evaporated. The resulting lipid film was dissolved in 100 µl of isopropanol (IPA):hexane:100 mM $NH_4COOH_{(aq)}$ 58:40:2 (mobile phase A) (16). Samples containing *n*-butanol were extracted similarly and 5 µl of 10 µg/ml 32:0 phosphatidylmethanol (PtdMeOH) was added as an internal standard. Mass spectrometric analysis and quantitation were performed essentially as previously described (17-19). MDS SCIEX 4000QTRAP hybrid triple quadrupole/linear ion trap mass spectrometer (Applied Biosystems, Foster City, CA) coupled to a Shimadzu HPLC system (Shimadzu Scientific Instruments, Inc., Columbia, MD) consisting of a SCL 10 APV controller, two LC 10 ADVP pumps, and a CTC HTC PAL autosampler (Leap Technologies, Carrboro, NC) was utilized for the analyses. Phospholipids were separated on a Phenomenex Luna Silica column (Phenomenex, Torrance, CA), (2 x 250 mm, 5 µm particle size) using a 20 µl sample injection. A binary gradient consisting of IPA:hexane:100 mM $NH_4COOH_{(aq)}$ 58:40:2 (mobile phase A) and IPA:hexane:100 mM $NH_4COOH_{(aq)}$ 50:40:10 (mobile phase B) was used for the separation. Instrumentation parameters and solvent gradient were previously described (18). Time courses were performed in two independent experiments each in triplicate. Statistical analysis was performed by two-way ANOVA with Bonferroni's post-test.

Spatial infection model - A spatial infection model for testing compound efficacy and influenza replication was adapted from (20). Monolayers of A549 cells were grown on chamber slides. A semisolid overlay made of agar and growth medium was allowed to cure on top of the monolayer. A Pasteur pipette was used to create a consistent reservoir in the overlay, and influenza virus was introduced through this reservoir. Cultures were then incubated at 37 °C for the duration of the infection.

RNA interference - A549 cells were transfected with 100nM siRNA (Ambion) specific to PLD isoforms using NeoFX (Ambion) and were subsequently infected with 1 MOI influenza A/Brisbane/59/2007 (H1N1) for 24 hours. Innate immune proteins were knocked down using 100 nM siRNA and the Neon Transfection System (Life Technologies). Knockdown was confirmed with gene specific TaqMan assays and the $2^{\Delta\Delta Ct}$ method using GAPDH to normalize alongside western blot to confirm loss of protein.

Immunofluorescence and live cell imaging - Samples were fixed in 4% formaldehyde, permeabilized with 0.3% Triton X-100, and then exposed to antisera targeting proteins of interest and corresponding fluorescent secondary antibodies alongside DAPI to visualize nuclei. Spatial infections were imaged and processed using Nikon C1Si and NIS Elements software. Confocal images were captured with a Zeiss LSM 510 NLO Meta and analyzed with Zeiss Zen 2011 software and ImageJ software (NIH). To determine colocalization, the PSC colocalization plugin was used to generate Pearson's and Spearman's coefficients. Briefly, NP and PLD2 signal channels were merged. Each Z slice was projected to maximum intensity. NP positive cells were masked, and the mask was used to determine if positive signal for each channel colocalized. Each mask was in excess of 20000 pixels to ensure a robust data set. Live cell imaging was performed

using spinning disc laser scanning confocal microscopy, carried out on a Marianas SDC imaging system (Intelligent Imaging Innocations/3i, Denver, CO) comprised of a CSU22 confocal scan head (Yokogowa Electric Corporation) and solid state lasers with wavelengths of 488 nm and 658 nm, configured on a motorized Axio Observer Z1 inverted microscope (Carl Zeiss MicroImaging) equipped with a Definite Focus system (Carl Zeiss) and spherical aberration correction optics. Time-lapsed 3-dimensional imaging was performed at 37 °C, 5% v/v CO_2 in a humidified atmosphere using an environmental control chamber (3i), and images acquired using a Plan-Apochromat 63x 1.4 NA oil objective on an Evolve 512 EMCCD (Photometrics, Tucson, AZ) using Slidebook 5.5 software (3i).

Animal infection - All animal studies were approved by the St. Jude Children's Research Hospital Animal Care and Use Committee (Protocol # 098), following the guidelines established by the Institute of Laboratory Animal Resources, approved by the Governing Board of the U.S. National Research Council. Female C57BL/6 mice (8-10 weeks old) were anesthetized and infected with indicated doses and strains of influenza A virus. Mice were weighed and monitored daily; tissues were collected at the specified times and kept at -80 °C until analysis. For drug treatment, mice were administered 13 mg/kg VU0364739 or vehicle (10% DMSO, 90% PEG) every 8 hours from day -1 to day 3 after infection or every 12 hours during the H7N9 study. All procedures were performed according to an institutionally-approved IACUC protocol, which includes a requirement for daily observation and euthanasia on detection of severe moribundity.

Titering - Infected animal lungs were titered using a standard plaque assay. Supernatant from infected cultures were titered using traditional $TCID_{50}$, and immunofluorescence was used to enumerate the number of infected cells in cultured samples.

Host gene expression - RNA was isolated from lungs and used in a reverse transcriptase PCR. The cDNA was then used in gene specific TaqMan assays to determine host gene expression, and the differences in expression were quantified using the $2^{\Delta\Delta Ct}$ method. The same amount of RNA was used in each reaction and samples were run in triplicate.

Statistical analysis - Quantitative data are presented as mean +/- SEM of at least three independent experiments.

RESULTS

Influenza infection potentiates PLD catalytic activity, and that activity is attenuated by VU0364739 treatment.- To determine the effect of influenza infection on PLD activity, human adenocarcinomic alveolar basal epithelial cells (A549) were infected with 1 MOI of human influenza strain A/California/04/2009 (H1N1) for 6 hours in the presence of 0.6% *n*-butanol. Instead of the typical biological nucleophile water, in the presence of a primary alcohol PLD will utilize the alcohol to produce a metabolically stable transphosphatidylation product, phosphatidylalcohol, as an alternative to hydrolysis producing PA. Figure 1*A* illustrates that influenza infection markedly stimulates PLD activity as measured by the increase in phosphatidylbutanol (PtdBuOH) production compared to cells that were not exposed to influenza virus (mock infected). Treatment with a PLD2-preferring inhibitor, VU0364739, is sufficient to block the influenza mediated PLD activity increase. As shown in Figure 1*B* both PLD1 and PLD2 are active during the viral entry phase and complete ablation of catalytic activity requires knockdown of both PLD1 and 2. This result suggests independent roles for both isoenzymes in entry.

Confocal microscopy based experiments were conducted to assess changes in the accumulation and localization of PLD during an influenza infection. A549 cells were grown on chamber slides and infected with 1 MOI influenza A/California/04/2009 (H1N1). Samples were fixed at 0, 30, 90, and 360 minutes post-infection, and were probed for influenza nucleoprotein (NP) and PLD2. PLD2 begins to accumulate at the

periphery of the cell as early as 30 minutes post-infection (Fig. 1*C*, *D*, and *E*). At the same time point, very low levels of NP were detected, also occurring at the outer reaches of the cell (Fig. 1*E*). PLD2 staining continued to intensify 90 and 360 minutes post-infection (Fig. 1*D*), and the observed PLD2 signal was increasing as well as moving from the cytoplasm to a perinuclear region (Fig. 1*E*). Influenza NP signal also intensified 360 minutes post-infection, and NP was moving from the cytoplasm (30 and 90 minutes post-infection) toward the nucleus (Fig. 1*D* and *E*). During the infection, PLD2 and NP were trafficking to similar subcellular locations. The extent of this colocalization was quantified. PLD2 and NP were increasingly colocalized at 30, 90, and 360 minutes post-infection (Fig. 1*C*) as measured by both Pearson's coefficient and rank correlation (Spearman). To further confirm that siRNA treatment was knocking down levels of PLD2 and that the PLD2 antibody was specific, we probed for PLD2 expression after infection of cells electroporated with control or PLD2 siRNA. We imaged more than 75 cells for each condition and found a consistent loss of 50% or more of stainable PLD2 in the siRNA treated cells (1*F*). Together, these data suggest PLD activity is stimulated by influenza infection, endogenous PLD redistributes during the infection, and the accumulation of PLD is occurring in the same subcellular location as influenza NP.

PLD is a targetable host factor that facilitates efficient influenza infection- To determine the role of PLD-mediated PA production in influenza infection, we employed a spatial infection model in the presence of 0.6% *n*-butanol with *tert*-butanol used as a negative control. This assay utilizes the use of primary alcohols as preferred nucleophiles in a PLD transphosphatidylation reaction as an assessment of exclusively PLD-produced PA.

Twenty-four hours post-infection infected cells were counted by anti-influenza NP staining (Fig. 2*A*). Infection with influenza strains A/Brisbane/59/2007 (H1N1), A/California/04/2009 (H1N1), or A/Brisbane/10/2007 (H3N2) resulted in fewer infected cells in the presence of *n*-butanol, indicating that blocking PLD production of PA substantially reduces the rate of cell to cell transmission of infection. Notably, averting the production of PLD-generated PA to PLD-generated PtdBuOH by use of primary alcohol, did not entirely prevent influenza infection but did significantly decrease the rate of infectious spread within the cultures.

In order to determine if PLD1 or PLD2 was preferentially required for efficient influenza infection, RNAi was employed to selectively knock down individual PLD isoforms. A549 cells were transiently transfected with siRNA that targeted PLD1 or PLD2, twenty-four hours prior to a 5 MOI influenza infection of A/Brisbane/59/2007 (H1N1). Twenty-four hours post-infection, a $TCID_{50}$ was used to measure influenza virus titers in culture supernatants (Fig. 2*B*). RNAi of either PLD1 or PLD2 inhibited influenza replication. However, the magnitude of the effect was greater with PLD2 knockdown. While each isoform appears to contribute to efficient influenza replication, the stronger inhibitory effects seen after PLD2 knockdown led us to focus on PLD2 inhibition and its effect on the host and viral replication for subsequent studies.

The development and optimization of the PLD inhibitors has been described (12), with the PLD2-preferring inhibitor, VU0364739 having a 75-fold selectivity for PLD2 over PLD1 (13). Based on previous studies, VU0364739 was used at 10 μM in all cell-based assays unless otherwise indicated (21). To demonstrate the importance of PLD2 during influenza replication another RNAi experiment was conducted while treating the PLD2-deficient cells with PLD2 inhibitor VU0364739. Viral titer was measured by $TCID_{50}$ after a 24 hour, 5 MOI influenza A/Brisbane/59/2007 (H1N1) infection. Pretreatment with VU0364739 for 1 hour caused a dramatic decrease in viral replication (Fig. 2*C*). Similar reductions in titer were also observed when PLD2 was knocked down by RNAi in vehicle treated samples. Finally, the specificity of this compound was confirmed by combining the apparent marginal, non-statistically significant additive nature of RNAi with VU0364739 treatment.

These observations were extended to establish the importance of PLD2 as a host factor required for infection by other clinically relevant strains of influenza. Pretreating cells for 1 hour with VU0364739 resulted in a significant decrease in the number of infected cells measured in the spatial infection assay with multiple viral strains at both 6- and 24- hours post-infection (Fig. 2*D*). Representative images of the spatial infection model assay (Fig. 2*E*) illustrate the reduction in influenza spread observed after VU0364739 treatment. PLD2 inhibition by VU0364739 effectively protected A549 cells from cell to cell spread of influenza, further demonstrating that PLD2 is required for efficient influenza infection and spread. A time-of-addition study was conducted where inhibitor was added over a time course spanning 2 hours before infection to 4 hours post-infection. Protection from infection was observed at all times of PLD inhibitor addition (data not shown).

Inhibition of PLD activity dramatically reduces influenza replication - The spatial infection model assay data was validated using the more traditional $TCID_{50}$ assay to assess viral reproduction *in vitro*. A549 cells were treated with 10 μM VU0364739 for 1 hour before infection, and the cells were then infected with the indicated doses and strains of influenza. At indicated time points, infectious supernatant was removed from the A549 cells and titrated on MDCK cells to measure viral reproduction. Using either a low MOI (Fig. 3*A*) or a high MOI (Fig. 3*B*) of influenza A/Brisbane/10/2007 (H3N2), a lower viral reproduction was observed when PLD2 was inhibited. In the case of the low MOI infection, viral titers were first noted to be lower at 16 hours post-infection and the effect was sustained 24 hours post-infection. Using the high MOI model, when A549 cells were treated with VU0364739, a significant reduction in viral reproduction was noted 12 hours post-infection and lasted through at least 24 hours.

The H3N2 strain used in our previous experiments is considered a low pathogenicity strain of influenza. To determine if host PLD is required for high pathogenicity and quickly replicating strains of influenza, VU0364739-treated A549 cells were infected with 0.01 MOI influenza rg-A/Vietnam/1203/2004 (H5N1) and viral reproduction was assessed during a more severe infection. Twenty-four hours post-infection, a massive decrease in viral titer was observed when PLD2 was inhibited during H5N1 infection (Fig. 3*C*). Subsequent investigation whether host PLD2 activity is required for infection using a recently emergent virus with pandemic potential, influenza strain A/Anhui/01/2013 (H7N9), was conducted. After 1 hour of 10 μM VU0364739 pretreatment, viral reproduction was effectively blocked 24 hours post-infection (Fig. 3*D*). Viral titer was near the limit of detection when PLD catalytic activity was inhibited, consistent with PLD2 being a host factor required for low and high pathogenicity influenza infections.

Using the same model, *in vitro* dose response experiments were perfomed using VU0364739 to determine the efficacy of the PLD2 inhibitor during H5N1 and H7N9 infection. A549 cells were treated for 1 hour with varying concentrations of VU0364739 before a 0.01 MOI infection of either influenza rg-A/Vietnam/1204/2004 or A/Anhui/1/2013. Supernatant was then used to measure viral reproduction in a $TCID_{50}$ assay 24 hours post-infection. In the case of the H5N1 infection, the IC_{50} of VU0364739 was calculated by non-linear regression analysis to be 2.1 μM (Fig. 3*E*). Similarly, the IC_{50} of VU0364739 was found to be 3.4 μM when cells were infected with an H7N9 influenza strain (Fig. 3*F*). These IC_{50} values are consistent with *in vitro* dose response experiments using influenza A/Brisbane/59/2007 (H1N1), A/Brisbane/10/2007 (H3N2), and A/California/04/2009 (H1N1) as well (data not shown). Based on these results, it was determined that inhibition of PLD2 can significantly lower influenza reproduction *in vitro*, and the decrease in viral titer occurs in a dose-dependent fashion.

PLD2-preferring inhibitor VU0364739 reduced viral titer in mouse lungs and delayed mortality during lethal H7N9influenza infection- Having shown that abrogation of PLD2 activity leads to a decrease in viral spread and reproduction *in vitro*, we wanted to determine if the loss of PLD2 could

reduce viral titer *in vivo*. Female C57BL/6 (B6) mice were treated intraperitoneally (IP) with dilutions of PLD2-preferring inhibitor VU0364739 every 8 hours from day -1 to 8 hours after infection with 1 LD_{50} (4000 EID_{50}) influenza A/Puerto Rico/8/1934 (H1N1) (PR8), administered intranasally on day 0. Due to solubility issues and observed acute vehicle toxicity, a long-term survival study with optimal dosing to achieve the therapeutic *in vivo* concentration continuously was not feasible at this time and viral titer was used as a readout to determine the role of PLD2 in a mouse model of influenza infection. Viral titer in lungs decreased significantly with PLD2 inhibitor VU0364739 treatment (Fig. 4*A*) and these protective effects were dose dependent. Additionally, to determine whether PLD2 inhibition could lead to lower viral titers in a more chronic situation, mice were given 13 mg/kg VU0364739 every 8 hours IP from day -1 to day 3 after infection. Animals treated with VU0364739 had significantly less viral replication in their lungs (Fig. 4*B*) on day 3. Concomitant with the decrease in viral titers, 8 hours after PR8 influenza infection significant upregulation of the innate immune proteins Mx1, OAS-L, and IFITM3 was observed when PLD2 was inhibited (Fig. 4*C*), indicating that the early immune response may be an important part of the mechanism of protection when mice are treated with VU0364739. IFITM3 has recently been described as a human restriction factor for influenza infection (22).

In order to identify survival benefits conferred by the observed reduction in viral titers, a study was conducted dosing mice with 13 mg/kg VU0364739 every 12 hours from day -1 to day 3 of a lethal influenza A/Anhui/1/2013 (H7N9) infection (Fig. 4*D*). Relative concentrations of the PLD inhibitor in various tissues of interest over time are presented in Fig. 4*E*. Administration of the PLD2-preferring inhibitor resulted in a modest, yet significant increase in survival and, in addition, delayed mortality (Fig. 4*D*). Although 80% of the mice administered VU0364739 eventually succumb, death occurs considerably later after infection (compared to influenza infected mice administered vehicle), clearly providing an extended window for further supportive therapy in a clinical setting. This demonstrates that by inhibiting PLD activity in the mouse, viral replication is decreased, and antiviral responses are upregulated leading to some protective benefits during a lethal influenza infection. No significant toxicity or neurological impairment was noted in rats receiving identical treatment (Tables 1 and 2). This inhibitor is a preclinical compound that has not been optimized for pharmacokinetic nor pharmacodynamic properties, and yet it demonstrates robust effects on viral spread and reproduction.

PLD2 inhibition alters endocytosis kinetics and aggregation of endocytic proteins- Inhibition of PLD function has been shown to decrease uptake of ligands in various systems (9,23,24). Given that perturbation of influenza virus trafficking during the early infection process can lead to degradation of the entering virus (11), it was hypothesized that PLD inhibition during influenza infection led to alterations of entry events which occur in the first minutes of infection. To support this hypothesis, the effect of PLD2 inhibition on normal endocytosis rates was assessed using the established transferrin uptake model, a classic demonstration of a clathrin-dependent trafficking process.

A549 cells pretreated with VU0364739 were labeled with fluorescent transferrin at 4 °C for 1 hour then placed into a heated microscope for live cell imaging. Images were recorded for one hour, and the frame and time of the transferrin fluorescence disappearance was noted (Fig. 5*A* and *B*). Cells treated with vehicle control were able to take up, traffic, and degrade transferrin by the 14^{th} frame, corresponding to an average time of 26 minutes after warming. In contrast, cells treated with VU0364739 took approximately 56 minutes to process the fluorescent ligand. These data indicate that inhibiting PLD2 activity with VU0364739 alters trafficking kinetics by extending the endocytosis process, rather than acting as a strict blockade.

Influenza entry is not entirely dependent on clathrin-mediated endocytosis, but it is widely accepted that the majority of incoming viruses enter via clathrin-dependent events, primarily by

the *de novo* formation of clathrin coated pits on the cell surface after exposure to influenza virus (225). After entry, influenza virus needs to be properly trafficked from the membrane to the nucleus. Along the way, the endosome is acidified (26), and the hemagglutinin protein undergoes a conformational change that creates a fusion pore between the viral and vesicle membranes through which viral ribonucleoproteins gain access to the cytoplasm, eventually entering the nucleus to initiate new virus production. The accumulation of trafficking associated proteins was visualized by confocal microscopy in A549 cells during a 0.05 MOI influenza A/California/04/2009 (H1N1) infection. Signal intensity and particle size were gated to determine protein accumulation. As proteins accumulate, the brightness and size of the fluorescence increases on a per cell basis. Clathrin recruitment was inhibited 50 minutes post-infection, and remained significantly lower (up to 80 minutes post-infection) with VU0364739 administration (Fig. 5*C*). During the first phase of viral entry, Rab5 accumulates on the early endosomes; however, in the presence of VU0364739 much less Rab5 accumulates 10 minutes post-infection (Fig. 5*D*). Similarly, VU0364739 treatment led to a significant reduction in recruitment of the late endosome marker CD63 90 minutes post-infection (Fig. 5*E*). Vesicular trafficking is also important for key elements of the late stages of viral replication and defects in Rab11 accumulation associated with viral protein trafficking to the membrane were consistently observed (data not shown). These data indicate that when PLD2 is inhibited during an infection, the normal cascade of protein accumulation required for proper endosomal maturation is disrupted, leading to inefficient trafficking of incoming virus particles, indicating that PLD2 is a host factor required for the efficient trafficking of influenza virus once within the cell.

Protection by PLD2 inhibition requires intact innate antiviral signaling- To assess whether the innate antiviral response was required for protection when cells are treated with the PLD2 inhibitor, an RNAi screen of essential innate immunity proteins *in vitro* was conducted. A549 cells were electroporated with 100 nM gene specific siRNA and infected with 5 MOI influenza A/Brisbane/10/2007 (H3N2) for 24 hours; decrease in protein expression was confirmed by Western blot analysis (data not shown). Viral titer was then measured using a traditional $TCID_{50}$ assay. A549 cells treated with control siRNA were protected by VU0364739 administration (Fig. 6*A*), showing a decrease in titer of 1.5 log units. However, VU0364739 treatment was not sufficient to protect cells transfected with siRNA targeting IRF3, Rig-I, or MxA. These three proteins are known to be vital to the innate defense against influenza. Interestingly, cells transfected with siRNA targeting the transcription factor IRF7 were still protected by VU0364739 treatment, but to a lower degree compared to cells transfected with control siRNA (0.9 log unit decrease in viral titer). These experiments demonstrate that altering trafficking kinetics with a PLD2 inhibitor alone was insufficient for complete protection from influenza infection. Cells need an intact antiviral response to attack and neutralize the invading virus, suggesting that PLD2 plays a critical role in the temporal-spatial regulation of endocytosis and innate antiviral sensing/defense during influenza infection. Disruption of PLD2 regulation of these events affords the host cell more time to detect the virus and mount an immune response.

One potential benefit of the delayed trafficking kinetics is the greater window allowed for innate immune interference during influenza infection. A key component of the innate response in the respiratory epithelium is MxA, a cytoplasmic dynamin-like GTPase, which is transcriptionally induced to high levels as part of the Type I IFN response, but is also found at basal levels in resting cells. MxA can interfere with early virus replication events by binding to viral NP (27). MxA recruitment was measured in A549 cells post-infection by the same manner employed to measure the endosomal markers. When PLD2 is inhibited during infection, MxA is observed to accumulate in foci at significant levels as early as 30 minutes post-infection (Fig. 6*B* and *C*). These data support a model whereby the slower rate of endocytosis following PLD2 inhibition allows cells more time to detect and respond to incoming influenza virus. Afforded this additional time, PLD inhibitor treated host cells are able to mount an immune response of greater magnitude and efficacy to neutralize the incoming virus, thus

promoting survival of the cell and protection from degradation of the invading virus.

DISCUSSION

PLD has been identified as a host restriction factor for influenza virus replication, and PLD catalytic activity is stimulated by influenza infection that colocalizes with NP positive staining structures over time. In addition, PLD2 functions to facilitate rapid endosomal trafficking, allowing the virus to escape an otherwise effective innate antiviral response. This response depends on RIG-I, IRF3, and the well-known antiviral protein MxA, but is largely independent of the antiviral targets of IRF7. Importantly, this work identifies a host cell process exploited by the virus to maximize its reproductive capacity and accelerate life cycle kinetics, allowing the pathogen to escape innate immune detection and neutralization.

The roles of PLD in endosomal trafficking are well documented (9,10). One advantage of targeting the PLD isoenzymes of host cells as an experimental antiviral strategy is that minimal evolution pressure would be exerted on the virus, which would otherwise encourage mutation and variant viral escape. Importantly, these enzymes have been shown to be nonessential to animal survival when either the PLD1 or PLD2 genes are knocked out (28,29). While the amount of PA generated by PLD2 alone may not be a significant fraction of the total cellular PA pool, discrete processes are likely to be linked to individual sources of PA-PLD2. For example, Yang et al. (30) reported that PLD2 was involved in opioid receptor endocytosis via a PA-p38 MAPK pathway. This may explain the negligible levels of toxicity observed using VU0364739 *in vivo*.

PA serves a multitude of roles in membrane biogenesis and curvature as well as cellular signaling, and has the potential to facilitate viral entry, replication, and egress. A detailed lipidomic analysis demonstrated that cytomegalovirus infection elicited a robust generation of PA in human fibroblasts (16). It is also interesting to note that PKC is a direct regulator of PLD activity and the role of PKC in influenza virion transport (11) through the late endosome may include some as yet unelucidated role for PLD. A more recently described PLD isoform known as PLD3 or HuK4 is related by sequence homology to p37, an essential protein in vaccinia virus. Although this PLD isoenzyme is not as well characterized, genetic variants in PLD3 were recently found to be of predictive value for risk in Alzheimer's disease (31). Overexpression of PLD3 leads to a significant decrease in intracellular amyloid-β-precursor protein and extracellular Aβ42 and Aβ40. Although human PLD3 cannot complement a p37 deficient vaccinia virus (32) primary alcohols similarly inhibit its function and its localization in the endoplasmic reticulum, suggesting some conservation of function. These recent discoveries provide further evidence that lipid signaling is a central process in many disease states. The identification of a role for PLD in influenza entry and innate immune escape expands our understanding that host cell signaling lipases have diverse and essential roles in viral infection and potentially offer a new series of therapeutic targets for pharmacological intervention.

Influenza virus, and potentially other enveloped viruses, are hijacking the endosomal compartments of infected host cells to hide from detection and to safely mature to a state that is favorable for efficient viral infection. Inhibition of PLD2 appears to alter the temporal spatial kinetics of this process. Despite the mode of entry, there is consensus that influenza virus must gain access to an endosome and be sorted to late endosomes with lower pH environments to undergo viral membrane-host membrane fusion. Our data suggest that when PLD2 is inhibited, endosomal sorting occurs more slowly than normal. We chose to stain clathrin, Rab5 and CD63 to elucidate well known markers of intracellular trafficking. Taken together the results suggest that PLD2 inhibition perturbs multiple pathways of influenza entry. The findings suggest that these proteins are accumulating more slowly when PLD2 is inhibited. Interestingly, PLD has been noted to be involved in various trafficking paradigms including clathrin, caveolin, and macropinocytosis (33,34,35). By shifting the kinetics of influenza trafficking much less viral spread was observed using the spatial infection model method and reduced viral replication using the traditional $TCID_{50}$ and plaque assays.

Concomitant with the shift in influenza trafficking, accumulation of antiviral sensors and effectors was observed. The protective mechanism is dependent on the innate immune system, indicating that the invading virus can be detected and the immune response mounted before it can begin an efficient infection. The inhibition of PLD effectively alters the host factor required by influenza to allow the infected cell to defend itself. Using the transferrin uptake model, the precise kinetics of ligand trafficking were defined and it was demonstrated that without PLD function, these events take approximately twice as long.

Recent development of isoform-preferring PLD inhibitors (12) presented an opportunity to disrupt the formation of PA by PLD and interrogate each isoenzyme's contribution during influenza infection. Based on the results using small molecule inhibitors and RNAi, PLD2 is proposed as a host factor that is used for efficient influenza infection. Importantly, our data suggest that PLD1 also plays a role in influenza infection. PLD1 RNAi can inhibit influenza replication. The focus on PLD2 over PLD1 in this study stems from interests in viral entry and host factors that are exploited by influenza to gain entry. Because of their subcellular location, PLD1 associates with the Golgi complex while PLD2 is distributed in the cell membrane. Hence, PLD2 regulation would be more relevant during entry whereas PLD1 would have a role in viral egress, assembly, and budding (9) The role of PLD1 and its relationship to the signaling pathways in which PLD2 are also involved is an important area for future studies.

The PLD2 pathway is a potentially attractive target for development of therapeutic agents, as minimal toxicity was observed from the administration of VU0364739 alone (any toxicity *in vivo* was associated with the vehicle and no *in vitro* toxicity was observed), and knocking out PLD2 in a mouse model is not obviously deleterious. Additional research is necessary to decode how host factors are co-opted by viruses to aid their pathogenesis, and the intervention necessary to prevent or minimize efficient viral infection. Since no current therapeutic alone is capable of completely protecting against influenza infection, future studies are required to evaluate the intriguing possibility that combinations of antiviral agents which work via distinct mechanisms could afford protection.

REFERENCES

1. Rossman, J.S., Jing, X., Leser, G.P., and Lamb, R.A. (2010) Influenza virus M2 protein mediates ESCRT-independent membrane scission. *Cell* **142**, 902–913.
2. Blanc, M., Hsieh, W.Y., Robertson, K.A., Kropp, K.A., Forster, T., Shui, G., Lacaze, P., Watterson, S., Griffiths, S.J., Spann, N.J., et al. (2013) The transcription factor STAT-1 couples macrophage synthesis of 25-hydroxycholesterol to the interferon antiviral response. *Immunity* **38**, 106–118.
3. Morita, M., Kuba, K., Ichikawa, A., Nakayama, M., Katahira, J., Iwamoto, R., Watanebe, T., Sakabe, S., Daidoji, T., Nakamura, S., et al. (2013) The lipid mediator protectin D1 inhibits influenza virus replication and improves severe influenza. *Cell* **153**, 112–125.
4. Tam, V.C., Quehenberger, O., Oshansky, C.M., Suen, R., Armando, A.M., Treuting, P.M., Thomas, P.G., Dennis, E.A., and Aderem, A. (2013) Lipidomic profiling of influenza infection identifies mediators that induce and resolve inflammation. *Cell* **154**, 213–227.
5. Ehrhardt, C., Marjuki, H., Wolff, T., Nürnberg, B., Planz, O., Pleschka, S., and Ludwig, S. (2006) Bivalent role of the phosphatidylinositol-3-kinase (PI3K) during influenza virus infection and host cell defence. *Cell Microbiol* **8**, 1336-1348
6. Chen, C. and Zhuang, X. (2008) Epsin 1 is a cargo-specific adaptor for the clathrin-mediated endocytosis of the influenza virus. *PNAS* **105**, 11790-11495
7. Carrasco, M., Amorim, M.J., and Digard, P. (2004) Lipid raft-dependent targeting of the influenza A virus nucleoprotein to the apical plasma membrane. *Traffic* **12**, 979-992.

8. Campbell, S.M., Crowe, S.M., and Mak, J. (2001) Lipid rafts and HIV-1: from viral entry to assembly of progeny virions. *J Clin Virol* **22**, 217-227
9. Roth, M.G. (2008) Molecular mechanisms of PLD function in membrane traffic. *Traffic* **9**, 1233–1239.
10. Selvy, P.E., Lavieri, R.R., Lindsley, C.W., and Brown, H.A. (2011) Phospholipase D: enzymology, functionality, and chemical modulation. *Chem. Rev.* **111**, 6064–6119.
11. Sieczkarski, S.B., Brown, H.A., and Whittaker, G.R. (2003) Role of protein kinase C {beta}II in influenza virus entry via late endosomes. *J. Virol.* **77**, 460–469.
12. Scott, S.A., Selvy, P.E., Buck, J.R., Cho, H.P., Criswell, T.L., Thomas, A.L., Armstrong, M.D., Arteaga, C.L., Lindsley, C.W., and Brown, H.A. (2009) Design of isoform-selective phospholipase D inhibitors that modulate cancer cell invasiveness. *Nat. Chem. Biol.* **5**, 108–117.
13. Lavieri, R.R., Scott, S.A., Selvy, P.E., Kim, K., Jadhav, S., Morrison, R.D., Daniels, J.S., Brown, H.A., and Lindsley, C.W. (2010) Design, synthesis, and biological evaluation of halogenated N-(2-(4-Oxo-1-phenyl-1,3,8-triazaspiro[4.5]decan-8-yl)ethyl)benzamides: Discovery of an isoform-selective small molecule phospholipase D2 inhibitor. *J. Med. Chem.* **53**, 6706–6719.
14. Scott, S.A., Mathews, T.P., Ivanova, P.T., Lindsley, C.W., Brown, H.A. (2014) Chemical modulation of glycerolipid signaling and metabolic pathways. *Biochim. Biophys. Acta – Mol. Cell Biol. Lipids* **1841,** 1060-1084.
15. Bligh, E.G., and Dyer, W.J. (1959) A rapid method of total lipid extraction and purification. *Can. J. Biochem. Physiol.* **37**, 911–917.
16. Liu, S.T.H., Sharon-Friling, R., Ivanova, P., Milne, S.B., Myers, D.S., Rabinowitz, J.D., Brown, H.A., and Shenk, T. (2011) Synaptic vesicle-like lipidome of human cytomegalovirus virions reveals a role for SNARE machinery in virion egress. *Proc. Natl. Acad. Sci. U. S. A.* **108**, 12869–12874.
17. Brown, H.A., Henage, L.G., Preininger, A.M., Xiang, Y., and Exton, J.H. (2007) Biochemical analysis of phospholipase D. *Methods Enzymol.* **434**, 49–87.
18. Ivanova, P.T., Milne, S.B., Byrne, M.O., Xiang, Y., and Brown, H.A. (2007) Glycerophospholipid identification and quantitation by electrospray ionization mass spectrometry. *Methods Enzymol.* **432**, 21–57.
19. Myers, D.S., Ivanova, P.T., Milne, S.B., and Brown, H.A. (2011) Quantitative analysis of glycerophospholipids by LC-MS: acquisition, data handling, and interpretation. *Biochim. Biophys. Acta- Mol. Biol. Lipids* **1811**, 748–757.
20. Lam, V., Duca, K.A., and Yin, J. (2005) Arrested spread of vesicular stomatitis virus infections in vitro depends on interferon-mediated antiviral activity. *Biotechnol. Bioeng.* **90**, 793–804.
21. Scott, S.A., Xiang, Y., Mathews, T.P., Cho, H.P., Myers, D.S., Armstrong, M.D., Tallman, K.A., O'Reilly, M.C., Lindsley, C.W., and Brown, H.A. (2013) Regulation of phospholipase D activity and phosphatidic acid production after purinergic (P2Y6) receptor stimulation. *J. Biol. Chem.* **288**, 20477–20487.
22. Everitt, A.R., Clare, S., Pertel, T., John, S.P., Wash, R.S., Smith, S.E., Chin, C.R., Feeley, E.M., Sims, J.S., Adams, D.J., et al. (2012) IFITM3 restricts the morbidity and mortality associated with influenza. *Nature* **484**, 519–523.
23. Antonescu, C.N., Danuser, G., and Schmid, S.L. (2010) Phosphatidic acid plays a regulatory role in clathrin-mediated endocytosis. *Mol. Biol. Cell* **21**, 2944-2952.
24. Corrotte, M., Chasserot-Golaz, S., Huang, P., Du, G., Ktistakis, N.T., Frohman, M.A., Vitale, N., Bader, M.-F., and Grant, N.J. (2006) Dynamics and function of phospholipase D and phosphatidic acid during phagocytosis. *Traffic* **7**, 365–377.
25. Lakadamyali, M., Rust, M.J., and Zhuang, X. (2004) Endocytosis of influenza viruses. *Microbes Infect.* **6**, 929–936.
26. Skehel, J.J., Cross, K., Steinhauer, D., and Wiley, D.C. (2001) Influenza fusion peptides. *Biochem. Soc. Trans.* **29**, 623–626.

27. Verhelst, J., Parthoens, E., Schepens, B., Fiers, W., and Saelens, X. (2012) Interferon-inducible Mx1 protein inhibits influenza virus by interfering with functional viral ribonucleoprotein complex assembly. *J. Virol.* **86**, 13445-13455.
28. Elvers, M., Stegner, D., Hagedorn, I., Kleinschnitz, C., Braun, A., Kuijpers, M.E.J., Boesl, M., Chen, Q., Heemskerk, J.W.M., Stoll, G., et al. (2010) Impaired {alpha}IIb{beta}3 integrin activation and shear-dependent thrombus formation in mice lacking phospholipase D1. *Sci. Signal.* **3**, ra1.
29. Oliveira, T.G., Chan, R.B., Tian, H., Laredo, M., Shui, G., Staniszewski, A., Zhang, H., Wang, L., Kim, T.-W., Duff, K.E., et al. (2010) Phospholipase D2 ablation ameliorates Alzheimer's disease-linked synaptic dysfunction and cognitive deficits. *J. Neurosci.* **30**, 16419 –16428.
30. Yang, L., Seifert, A., Wu, D., Wang, X., Rankovic, V., Schröder, H., Brandenburg, L.O., Höllt, V., and Koch, T. (2010) Role of phospholipase D2/phosphatidic acid signal transduction in micro- and delta-opioid receptor endocytosis. *Mol. Pharmacol.* **78**, 105–113.
31. Cruchaga, C., Karch, C.M., Jin, S.C., Benitez, B.A., Cai, Y., Guerreiro, R., Harari, O., Norton, J., Budde, J., Bertelsen, S., et al. (2013) Rare coding variants in the phospholipase D3 gene confer risk for Alzheimer's disease. *Nature* **505**, 550-554.
33. Munck, A., Böhm, C., Seibel, N.M., Hashemol Hosseini, Z., and Hampe, W. (2005) Hu-K4 is a ubiquitously expressed type 2 transmembrane protein associated with the endoplasmic reticulum. *FEBS J.* **272**, 1718–1726.Padron, D., Tall, R.D., and Roth, M.G. (2006) Phospholipase D2 is required for efficient endocytic recycling of transferrin receptors. *Mol Biol Cell* **17**, 598-606
34. Czarny, M., Fiucci, G., Lavie, G., Banno, Y., Nozawa, Y., and Liscovitch, M. (2000) Phospholipase D2: functional interaction with caveolin in low-density membrane microdomains. *FEBS Letters* **467**, 326-332.
35. Manhankali, M., Peng, H.J., Cox, D., and Gomex-Cambronero, J. (2011) The mechanism of cell membrane ruffling relies on a phospholipase D2 (PLD2), Grb2 and Rac2 association. *Cell Signal* **23**, 1291-1298.

Acknowledgments - We thank Pavlina T. Ivanova, Stephen B. Milne, and David S. Myers for contributions to the mass spectrometry analysis of glycerophospholipid composition changes, Lana McClaren and Christine M. Oshansky for support in the lipid analysis and viral titer experiments, Michelle D. Armstrong for technical support and assistance with preparation of the manuscript, the Cell & Tissue Imaging Center at St. Jude Children's Research Hospital, Paul Digard and T. David K. Brown for assistance with microscopy and helpful conversations.

FOOTNOTES

*Partial support for this work was provided from the National Institutes of Health (U54MH084659, P01ESO013125, NIAID HHSN2722008000058C, NIH HHSN266200700005C) and Medical Research Council grant (RG53985).

To whom correspondence should be addressed: H. Alex Brown*, Departments of Pharmacology, Vanderbilt University Medical Center Vanderbilt University, Nashville TN 37232, USA, Tel.: (615) 936-3888, E-mail: alex.brown@vanderbilt.edu; Paul G. Thomas**, Department of Immunology, St. Jude Children's Research Hospital, Memphis, TN 38105, USA, Tel.: (901) 595-6507, E-mail: Paul.Thomas@stjude.org

[1]Department of Immunology, St. Jude Children's Research Hospital, Memphis, TN 38105-3678, USA,
[2]Department of Biological Sciences, University of Memphis, Memphis, TN 38152, USA,

[3]Department of Veterinary Physiology and Biochemistry, Lala Lajpat Rai University of Veterinary and Animal Sciences, Hisar- 125004 , Haryana, India
[4]Department of Pathology, University of Cambridge, Cambridge, UK CB2 1QP,
[5]Department of Pharmacology, Vanderbilt University Medical Center, Nashville, TN 37232-6600, USA,
[6]Department of Chemistry and The Vanderbilt Institute of Chemical Biology, Vanderbilt University, Nashville, TN 37232, USA,
[7]Department of Biochemistry, Vanderbilt University Medical Center, Nashville, TN 37232-6600, USA,
[8]Vanderbilt Center for Neuroscience Drug Discovery, Vanderbilt University Medical Center, Nashville, TN 37232-0697, USA
[9]The abbreviations used are: PLD, phospholipase D; PC, phosphatidylcholine; PA, phosphatidic acid; HA, hemagglutinin receptor; PKC, protein kinase C; PtdBuOH, phosphatidylbutanol; NP, nucleoprotein; IP, intraperitoneally.

FIGURE LEGENDS

FIGURE 1. Influenza infection stimulates PLD activity. ***A.*** A549 cells treated for one hour with or without 10 μM PLD inhibitor VU0364739 were then infected for one hour with 1 MOI influenza A/California/04/2009 (or mock infected), after which the inoculum was removed. The cells were cultured for 6 hours in the presence of 0.6% *n*-butanol. PLD activity as a measure of phosphatidylbutanol (PtdBuOH) was determined in cell lysates by mass spectrometrometric analysis. ***B***. RNAi of PLD1, PLD2 or PLD1&2. A549 cells were transfected with isoform specific siRNA 1 day before a 5 MOI infection of influenza A/Brisbane/59/2007 (H1N1). 30 minutes after infection, PLD catalytic activity measured in the same manner as (***A***). ***C, D*** and ***E.*** A549 cells were infected with 1 MOI influenza A/California/04/2009 (H1N1), and samples were fixed and probed for influenza nucleoprotein (NP) and PLD2 at 0, 30, 90, and 360 minutes after infection. Z-stacks of the infected cultures were collected using confocal microscopy, and ImageJ was used to determine PLD and influenza NP colocalization (***C***) during infection as well as protein accumulation (***D***). Quantification of the degree of correlation between NP and PLD shows that they significantly colocalize as early as 30 minutes post-infection, and the colocalization has the highest correlation coefficient 360 minutes post-infection. PLD2 signal begins to intensify 30 minutes after infection and continues to increase in both size and intensity throughout the duration of the infection. NP signal lags behind that of PLD2, but begins to intensify 90 and 360 minutes post-infection. ***E.*** Representative images from a 1 MOI influenza A/California/04/2009 (H1N1) infection taken 0, 30, 90, and 360 minutes post-infection. The green signal is influenza (NP), the magenta signal is PLD2, and the blue signal is DAPI staining, bar = 10 μm. As the infection progresses, PLD2 staining begins to accumulate at the cell periphery, then intensifies, and finally moves to a perinuclear region. NP staining first appears at the cell periphery and then intensifies in the nucleus. ***F.*** Representative images from PLD2 monoclonal antibody validation. A549 cells were electroporated with 100 nM scrambled control or PLD2 siRNA and left to rest for 24 hours. Cells were fixed 8 hours after a 1 MOI A/Brisbane/59/2007 (H1N1), green signal is influenza NP, red signal is PLD2, and blue signal is nuclei. All data are mean ± SEM.

FIGURE 2. PLD2 is required for efficient influenza infection and inhibition of PLD-generated PA by primary alcohol, RNAi or small molecule VU0364739 dramatically hinders cell to cell spread of influenza. ***A***. Number of influenza infected cells in cultures of A549 cells treated with 0.6% *tert*- or *n*-butanol for 1 hour prior to spatial infection by 1 MOI of the indicated influenza virus strain for 24 hours. Differences were assessed by t-test. ***B***. (upper) RNAi of PLD isoforms. A549 cells were transfected with siRNA targeting PLD1 or PLD2 24 hours prior to infection with 5 MOI influenza A/Brisbane/59/2007 (H1N1); 8 hours post-infection, influenza replication was measured by $TCID_{50}$. (lower) Immunoblot of

human PLD1 and PLD2 from A549 cells following RNAi treatment. Lysates were separated on 10% polyacrylamide gel, transferred to nitrocellulose overnight, and incubated with primary antibodies for PC-PLD1 (Santa Cruz sc-25512) or PLD2 (Abgent AT3337a). Immunoblots were developed with ECL western blotting substrate (Pierce cat# 32106). ***C.*** A549 cells were transiently transfected with PLD2 specific siRNA or scrambled control siRNA 24 hours before infection. An hour before infection, the cells were treated with DMSO or VU0364739 (10 μM). The cells were infected with 5 MOI A/Brisbane/59/2007 (H1N1) and influenza replication was measured by $TCID_{50}$ 24 hours after infection. Differences between amounts of infected cells as well as influenza replication were compared using a one-way ANOVA and Dunnett's post-test. ***D.*** Influenza spatial infection (following 1-hour 10 μM PLD2-preferring inhibitor VU0364739 pretreatment) with clinically relevant strains of influenza at 1 MOI. At both 6- and 24-hours post-infection, significantly fewer numbers of influenza-infected cells were counted in VU0364739 pretreated samples. Data was analyzed by t-test. ***E***. Representative fluorescent photomicrograph mosaics following a 24-hour spatial infection of A549 cells with influenza A/Brisbane/59/2007 (H1N1). Green signal is influenza infected cells and blue signal is DAPI staining, bar = 10 μm. All data are mean ± SEM.

FIGURE 3. Influenza replication is severely reduced when PLD2 is inhibited by VU034739. A549 cells were pretreated with 10 μM VU0364739 or DMSO for 1 hour, then infected with either: ***A***. Low 0.01 MOI H3N2 influenza, ***B***. High 5.0 MOI H3N2 influenza, ***C***. 0.01 MOI H5N1 influenza, or ***D***. 0.01 MOI H7N9 influenza for an hour at 4 °C, and then the infectious supernatant containing the virus was removed and titrated on MDCK cells to assess viral production at indicated times post-infection. Under PLD2 inhibitor treatment, poor viral replication in all influenza strains tested by 24 hours post-infection was observed, and the viral output defect was noted as early as 12 hours post-infection in the case of H3N2 and H7N9. Differences were assessed using a two-way ANOVA and Bonferroni's post-test, where * $p < 0.05$, ** $p < 0.01$, *** $p < 0.001$, **** $p < 0.0001$. ***E***. and ***F***. Dose response curves to determine the IC_{50} of VU0364739 on influenza titer after a 24 hour infection with (***E***) rg-A/Vietnam/1204/2004 (H5N1) or (***F***) A/Anhui/1/2013 (H7N9). A549 cells were treated with the indicated concentration of VU0364739 for one hour before infection, $TCID_{50}$ was used to measure viral load. All data are mean ± SEM.

FIGURE 4. PLD2 inhibitor decreased early viral titer in a dose dependent manner and delayed mortality in a lethal H7N9 model. ***A***. Mice treated with VU0364739 displayed lung viral titers that were drastically reduced 8 hours after 4000 EID_{50} PR8 influenza infection, and the reduction occurred in a dose-dependent manner. Data were compared by ANOVA and Bonferroni's post-test, with $N \geq 5$ mice used for each dose, ** $p < 0.01$. ***B***. Viral replication was similarly inhibited 3 days after 4000 EID_{50} PR8 influenza infection in mice treated with 13 mg/kg VU0364739 three times a day from day -1 to day 3 post influenza infection. Data were analyzed by t-test, ** $p < 0.01$. ***C***. RNA from PR8 influenza-infected lungs was isolated and gene expression was measured using TaqMan based qPCR 8 hours after infection. Innate immune proteins Mx1, OASL, and IFITM3 were significantly upregulated as early as 8 hours after infection, as measured by t-test, * $p < 0.05$, ** $p < 0.01$. ***D***. Mice receiving 13 mg/kg VU0364739 twice/day from day -1 to day 5 post-infection were inoculated with $10^{3.5}$ $TCID_{50}$ (1 LD_{50}) influenza A/Anhui/1/2013 (H7N9). The PLD2 inhibitor conferred a substantial delay in mortality and a 20% survival advantage, a significant benefit as measured by either Log-Rank test ($p = 0.0194$) or Gehan-Breslow-Wilcoxon test ($p = 0.0165$), * $p < 0.05$. ***E.*** Plasma, brain, lung and liver exposures following a single 10 mg/kg intraperitoneal dose of the PLD inhibitor VU0364739 in mouse. Samples were stored at -80 °C until extraction and LC-MS/MS analysis. (N = 2 samples per time point).

FIGURE 5. PLD inhibition alters ligand trafficking kinetics and accumulation of endocytosis regulatory proteins. ***A* & *B***. A549 cells were treated for 1 hour with DMSO or VU0364739 (10 μM) prior to being labeled for 1 hour at 4 °C with 100 nM AlexaFluor 647 – Transferrin. Live cell imaging (representative movies in supplemental) was used to assess the kinetics of transferrin uptake. To quantify this assay, both

the frame (*A*) and the time (*B*) were used to determine when the fluorescent signal disappeared, signaling recycling of transferrin. Live cell imaging was performed using Slidebook imaging software and frame time measurements were compared using t-tests, data are mean ± SEM. ***C*** **-** ***E***. A549 cells were treated for 1 hour with DMSO or VU0364739 (10 μM) then infected with 0.05 MOI influenza A/California/04/2009 (H1N1). Cells were stained and examined by confocal microscopy for the accumulation of: ***C***- Clathrin; ***D***- Rab5 (early endosome); ***E***- CD63 (late endosome). Less clathrin is recruited at 50 and 80 min post-infection under inhibitor treatment, and less Rab5 (***D***) and CD63 (***E***) accumulate after 10 and 90 min post-infection, respectively. In these experiments protein accumulation is defined by gating signal intensity as well as size such that higher y-axis values represent bigger and brighter foci of signal. A two-way ANOVA with Bonferroni's post-test was used to examine data from (***C***), * $p < 0.05$, ** $p < 0.01$, **** $p < 0.0001$; t-tests were used to analyze data from (***D***) and (***E***) with p-values indicated. Data are mean ± SEM.

FIGURE 6. Innate immune factors are required for PLD2 inhibitor mediated protection from influenza. ***A***. A549 cells were transfected with siRNA targeting effectors or transcription factors involved in the Type I IFN pathway, then subsequently infected with 5 MOI influenza A/Brisbane/10/2007 (H3N2) for 24 hours, and supernatant was titered on MDCK cells to measure viral reproduction. As a control viral replication was significantly reduced in cells transfected with scrambled siRNA and treated with PLD2 inhibitor. When cells lack IRF3, Rig-I or MxA, treatment with VU0364739 cannot protect against influenza infection. The innate requirements are restricted to IRF3 mediated signaling, as protection was afforded to cells with IRF7 knocked down. Representative Western blots are presented to confirm loss of protein expression after RNAi. ***B***. To demonstrate the robust innate antiviral response to influenza infection after PLD2 inhibition, A549 cells were infected with 1 MOI influenza A/California/04/2009 (H1N1) and levels of MxA were assessed by confocal microscopy 30 minutes post-infection. ***C***. MxA accumulates much more rapidly and to a much greater magnitude when PLD2 is inhibited. The dramatic MxA activity is visualized in representative images where green signal marks influenza NP, red signal is MxA, and blue signal is DAPI, bar = 10 μm. A two-way ANOVA with Bonferroni's post-test was used to examine data from (***A***), ** $p < 0.01$, **** $p < 0.0001$; a t-test was used to analyze data from (***B***). Data are mean ± SEM.

TABLE 1. Rat liver toxicity panel shows little effect of PLD inhibitor VU0364739. Only globulin and total protein showed higher levels with inhibitor treatment (N = 5 - 6 rats per treatment, $p < 0.05$ by Mann-Whitney test) and each were within normal clinical ranges for both the vehicle control and PLD inhibitor treatment groups. Principal components analysis of the z-score standardized values across the screening panel displayed no clustering of the multivariate results by treatment, and none of the principal components differed significantly either ($p > 0.05$ by t-test).

	Means ± sems		Units	P-value
	Vehicle	*VU0364739*		
Albumin	3.6±0.1	3.6±0.0	g/dL	0.5368
Alkaline phosphatase	212±11	207±13	U/L	0.7922
Alanine aminotransferase	102±8	113±5	U/L	0.5368
Amylase	1118±59	1142±41	U/L	0.6623
Blood urea nitrogen	12.0±2.0	15.6±1.5	mg/dL	0.0823
Calcium	10.8±0.2	11.0±0.2	mg/dL	0.3290
Creatinine	0.33±0.01	0.42±0.04	mg/dL	0.1255
Globulin	2.3±0.1	2.6±0.1	g/dL	0.0303
Glucose	143±7	141±5	mg/dL	0.7922
Potassium	5.72±0.42	5.72±0.15	mmol/L	0.6623
Sodium	139±2	142±1	mmol/L	0.3290
Phosphorus	8.8±0.2	9.0±0.2	mg/dL	0.5368
Total bilirubin	0.22±0.07	0.16±0.01	mg/dL	0.7922
Total protein	5.9±0.1	6.3±0.1	g/dL	0.0303

TABLE 2. PLD inhibitor VU0364739 is without effect in a Modified Irwin Neurological Battery in rats. Changes in the Modified Irwin Neurological Battery were evaluated using a rating scale from 0 to 2: 0, no effect; 1, modest effects; 2, robust effect. Male Harlan Sprague Dawley rats (N = 6, approximately 250 grams) were pretreated with vehicle alone or a 13 mg/kg IP dose of VU0364739 and then tested in the Irwin battery at 30 minutes after treatment and subsequently monitored for 8 hours.

Modified Irwin Neurological Battery with VU0364739					
Autonomic Nervous System					
Time	**30min**	**1hr**	**2hr**	**4hr**	**6hr**
Ptosis	0	0	0	0	0
Exophtalmus	0	0	0	0	0
Miosis	0	0	0	0	0
Mydriasis	0	0	0	0	0
Corneal reflex loss	0	0	0	0	0
Pinna reflex loss	0	0	0	0	0
Piloerection	0	0	0	0	0
Respiratory rate	0	0	0	0	0
Writhing	0	0	0	0	0
Tail erection	0	0	0	0	0
Lacrimation	0	0	0	0	0
Salivation	0	0	0	0	0
Vasodilatation	0	0	0	0	0
Skin color	0	0	0	0	0
Irritability	0	0	0	0	0
Loose Stool	0	0.25	0.5	0.4	0
Rectal temp. (°C)	37	37.3	37.4	37.2	37
Somatomotor systems					
Motor activity	0	0	0	0	0
Convulsions	0	0	0	0	0
Arch/roll	0	0	0	0	0
Tremors	0	0	0	0	0
Leg weakness	0	0	0	0	0
Rigid stance	0	0	0	0	0
Spraddle	0	0	0	0	0
Placing loss	0	0	0	0	0
Grasping loss	0	0	0	0	0
Righting loss	0	0	0	0	0
Catalepsy	0	0	0	0	0
Tail pinch	0	0	0	0	0
Escape loss	0	0	0	0	0

Figures.

Figure 1.

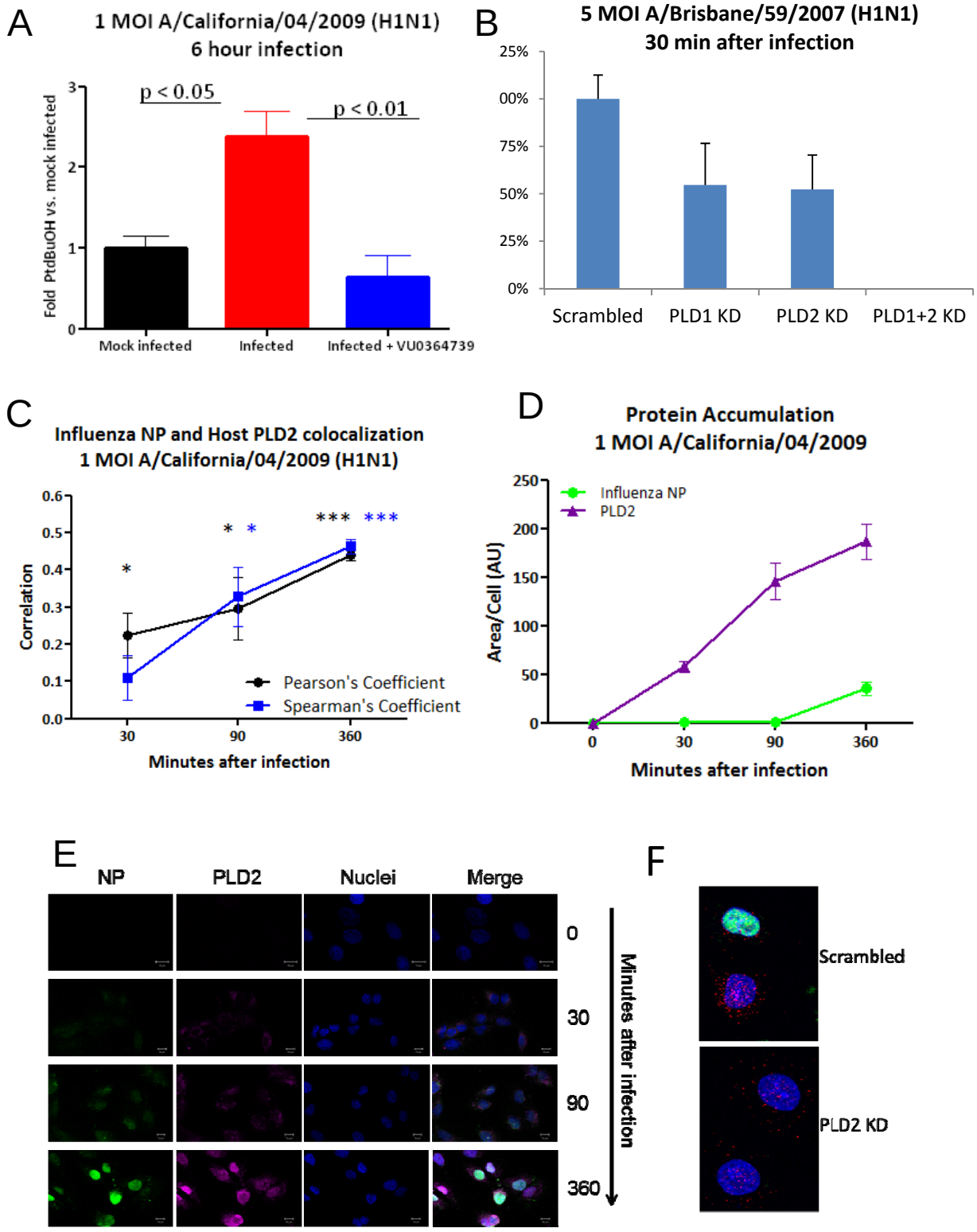

Figure 2.

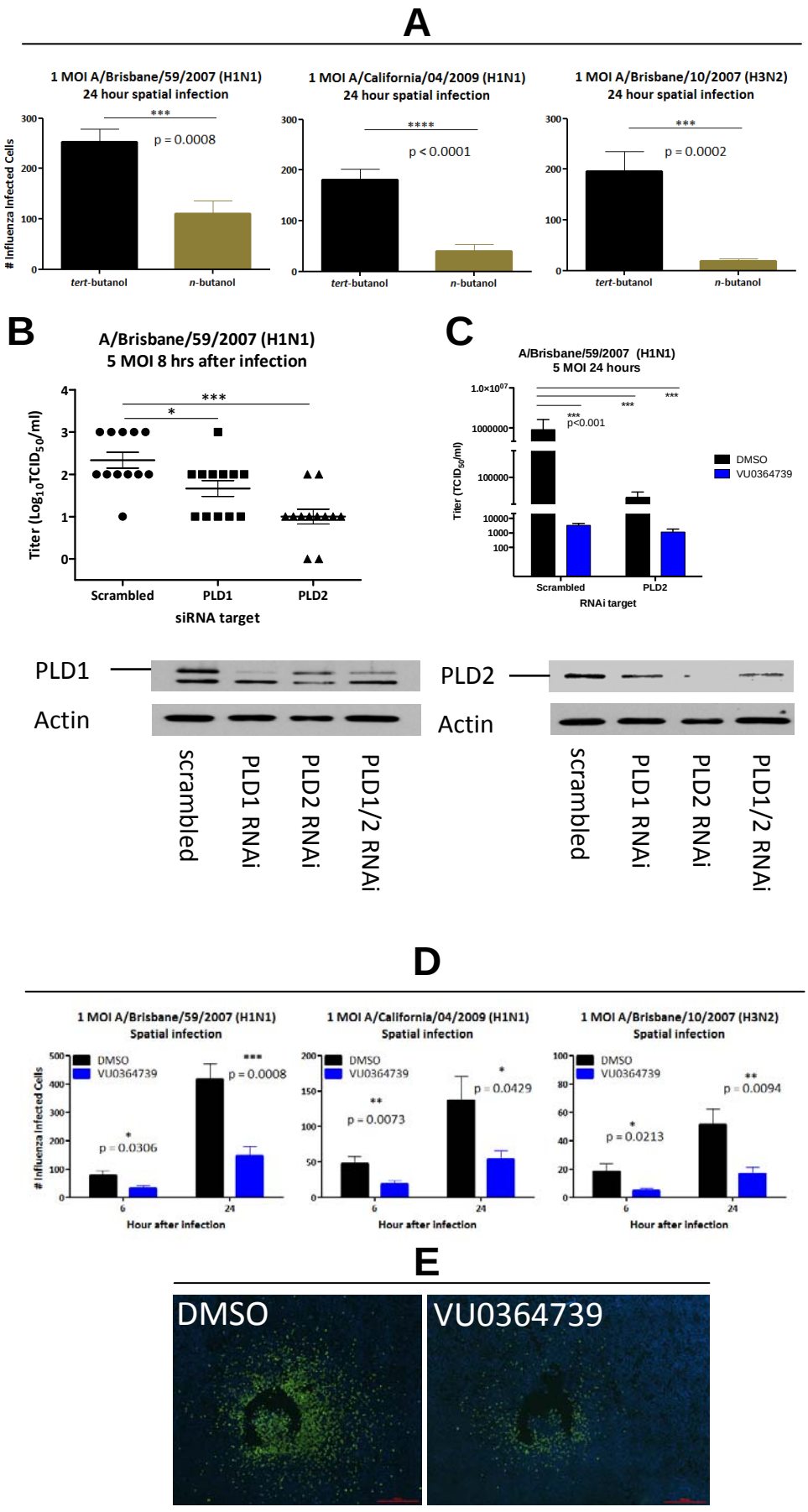

Figure 3.

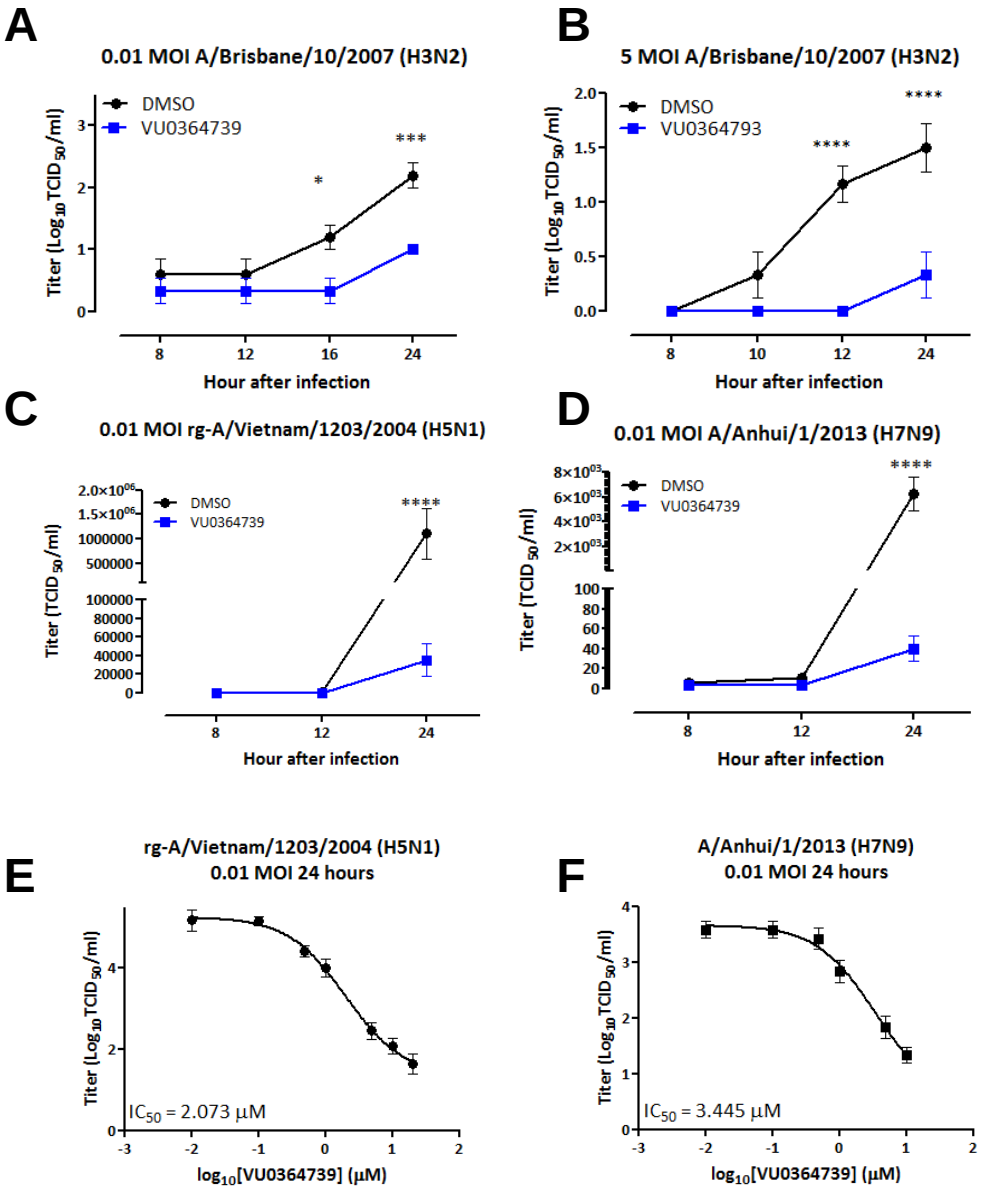

Figure 4.

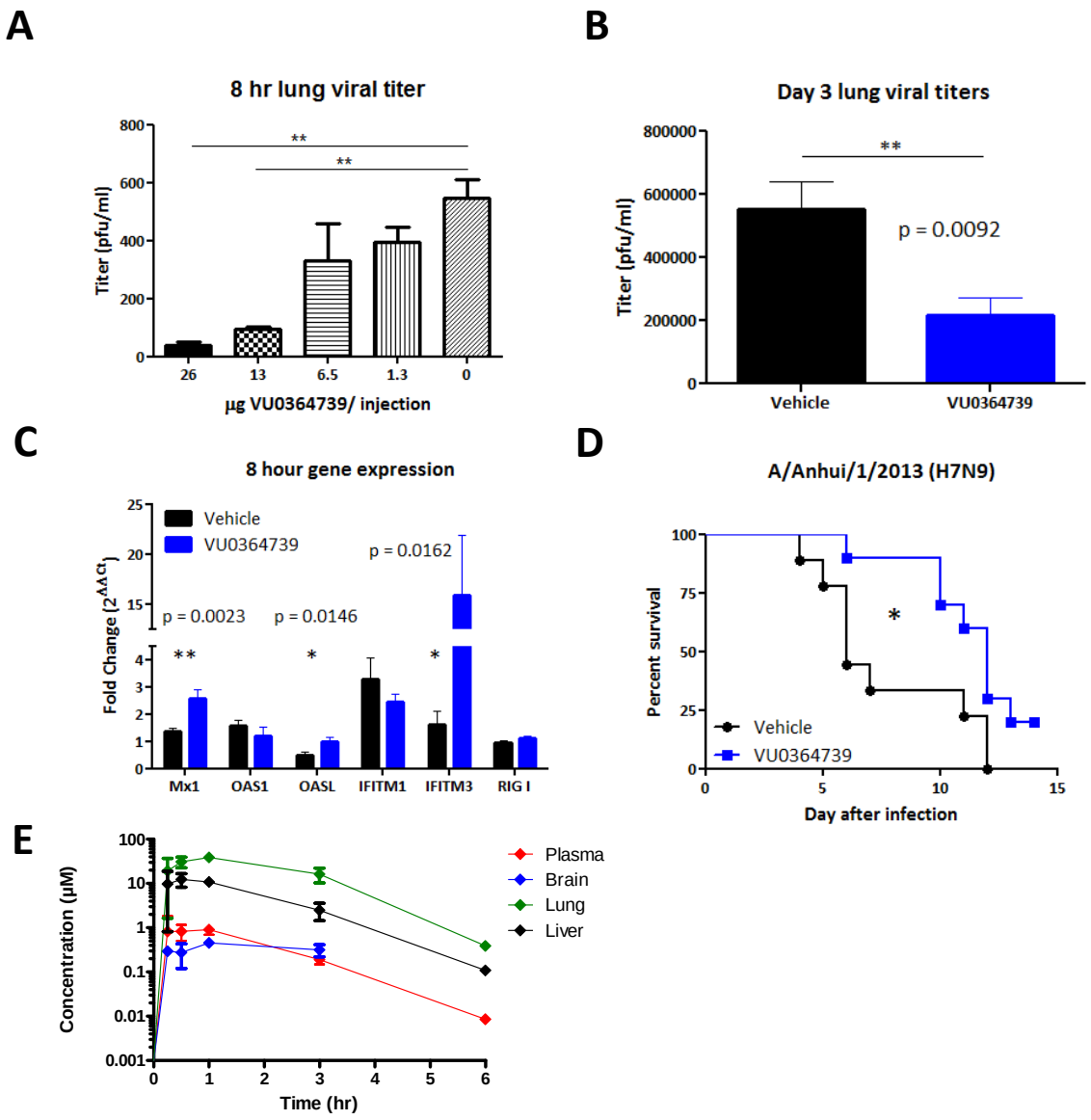

Figure 5.

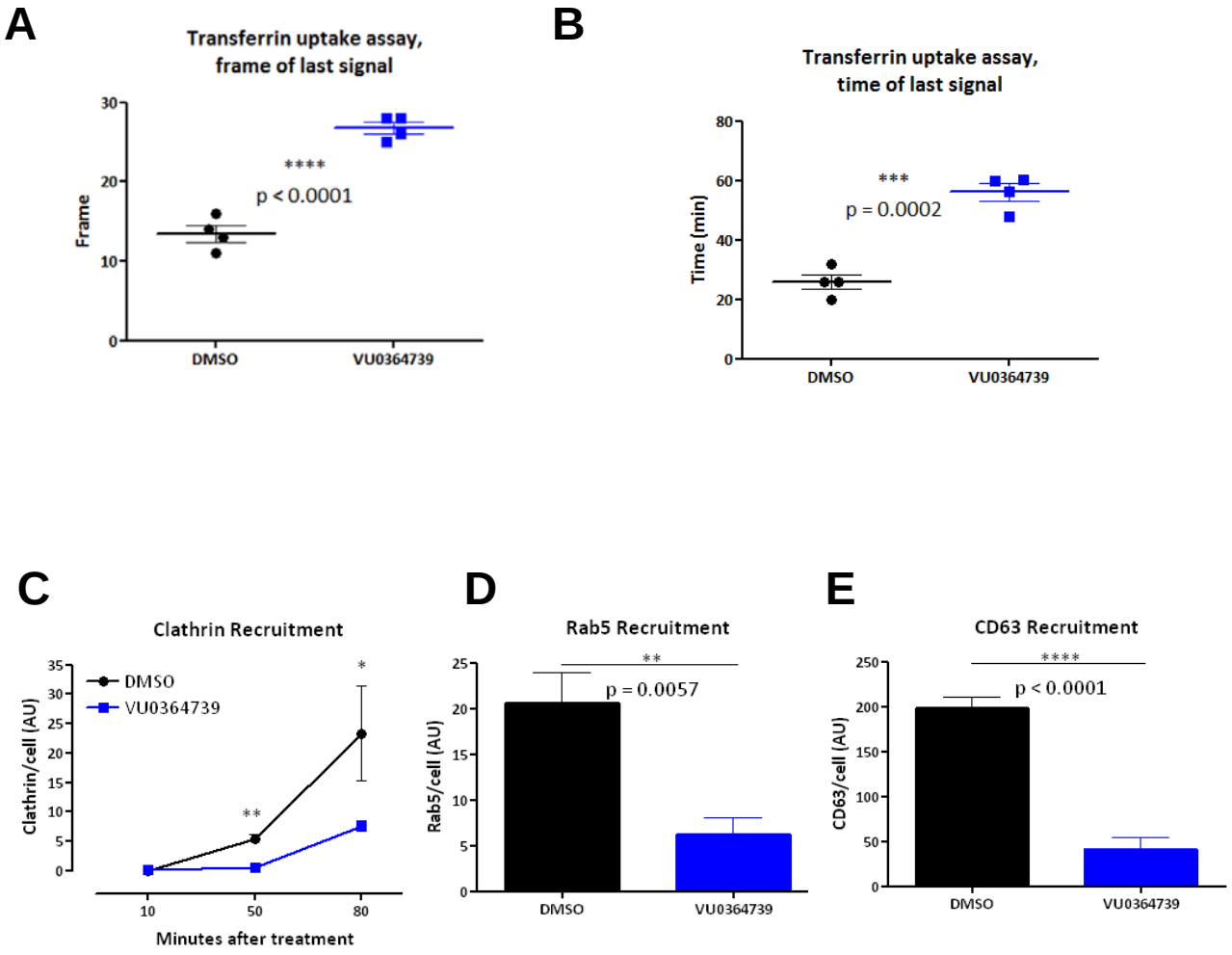

Figure 6.

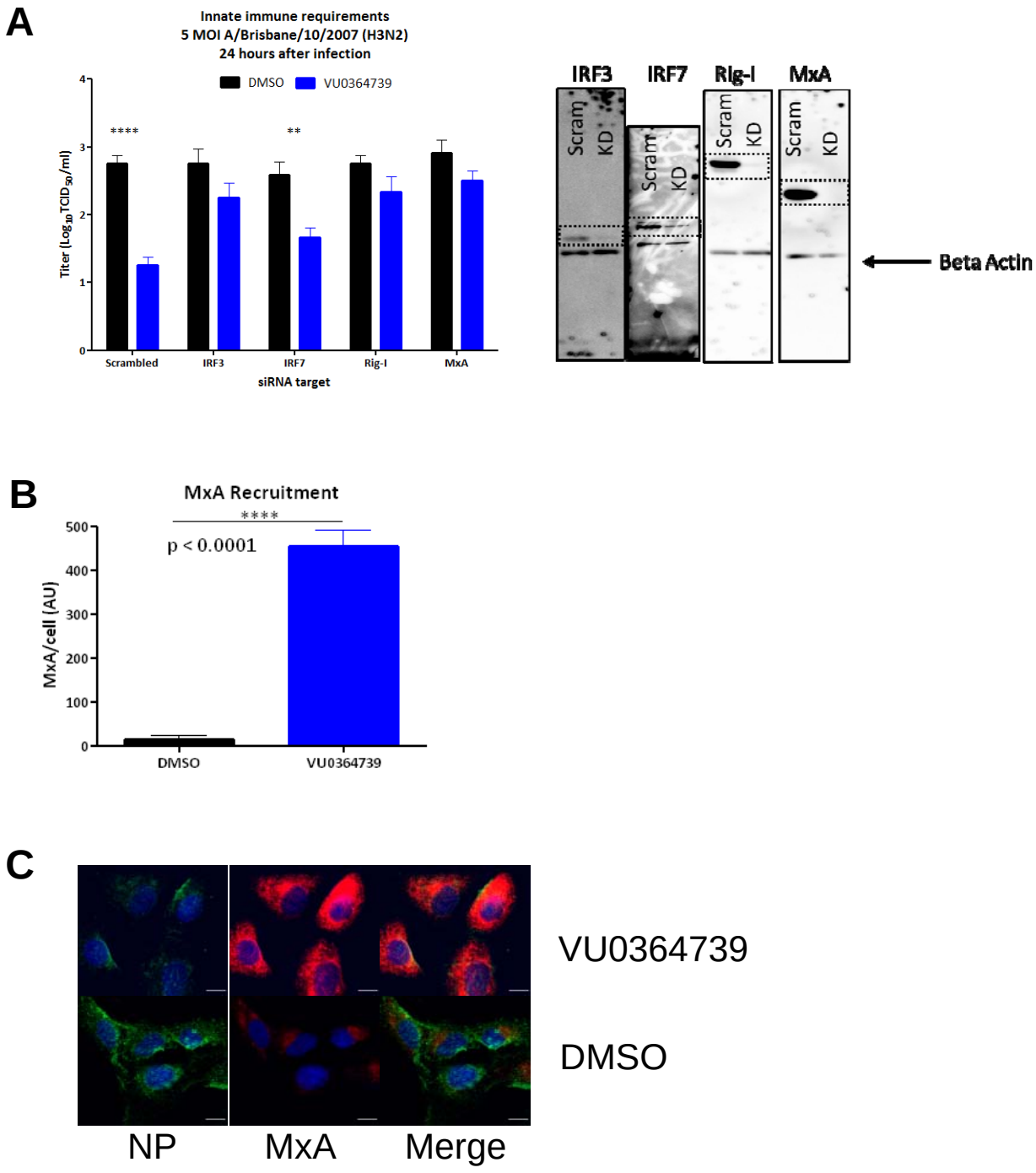

Phospholipase D facilitates efficient entry of influenza virus allowing escape from innate mmune inhibition

Thomas H. Oguin III, Shalini Sharma, Amanda D. Stuart, Susu Duan, Sarah A. Scott, Carrie K. Jones, J. Scott Daniels, Craig W. Lindsley, Paul G. Thomas and H. Alex Brown

J. Biol. Chem. published online July 27, 2014
